REVIEWS

Journal of Semiconductors
(2019) 40, 011801
doi: 10.1088/1674-4926/40/1/011801

Growth and fundamentals of bulk β-Ga_2O_3 single crystals

H. F. Mohamed[1, 2], Changtai Xia[1, †], Qinglin Sai[1], Huiyuan Cui[1], Mingyan Pan[1], and Hongji Qi[1]

[1]Key Laboratory of Materials for High Power Laser, Shanghai Institute of Optics and Fine Mechanics, Chinese Academy of Sciences, Shanghai 201800, China

[2]Physics Department, Faculty of Science, Sohag University, 82524, Sohag, Egypt

Abstract: The rapid development of bulk β-Ga_2O_3 crystals has attracted much attention to their use as ultra-wide bandgap materials for next-generation power devices owing to its large bandgap (~ 4.9 eV) and large breakdown electric field of about 8 MV/cm. Low cost and high quality of large β-Ga_2O_3 single-crystal substrates can be attained by melting growth techniques widely used in the industry. In this paper, we first present an overview of the properties of β-Ga_2O_3 crystals in bulk form. We then describe the various methods for producing bulk β-Ga_2O_3 crystals and their applications. Finally, we will present a future perspective of the research in the area in the area of single crystal growth.

Key words: β-Ga_2O_3; crystal structure; bulk crystal growth; applications

Citation: H F Mohamed, C T Xia, Q L Sai, H Y Cui, M Y Pan, and H J Qi, Growth and fundamentals of bulk β-Ga_2O_3 single crystals[J]. *J. Semicond.*, 2019, 40(1), 011801. http://doi.org/10.1088/1674-4926/40/1/011801

1. Introduction

Beta gallium oxide has attracted rapidly growing interest in the past decade and is considered a promising candidate for power device applications. Gallium oxide is a significant semiconductor oxide and has a large bandgap energy (~4.9 eV) with a decent mobility (~100 cm^2/Vs), a high breakdown strength (8 MV/cm), and good thermal stability. It was first studied in the 1950s, and its crystal structure was determined by Geller (1960)[1]. Ga_2O_3 has considerable potential in high-electric-field-strength and high-temperature applications owing to its wide bandgap. There exists an empirical relationship between the electrical breakdown value and semiconductor bandgap. A slight increase in the bandgap value can greatly improve the electric field strength (discussed in section 3.2). Therefore, Ga_2O_3 is an important candidate for high breakdown voltage devices. Bulk β-Ga_2O_3 single crystals have been successfully growth to large and high-quality crystals at a low production cost; this can make them competitive in the advancement technological applications. In this article, we briefly review the growth, doping, and application of β-Ga_2O_3 bulk single crystals. This article is divided into three main sections. The first section presents crystal structures and the electronic band structure. The second section presents the growth technique. The final section describes the role of the defects and impurities.

2. Crystal structure of β-Ga_2O_3

We discuss the crystal structure and electronic band structure of β-Ga_2O_3 and summarize the main points. Gallium oxide has a melting point of approximately 1800 °C, and five polymorphs named α, β, γ, δ, and ε exist in nature depending strictly on the preparation conditions[2]. Among these phases, β-Ga_2O_3 is the most thermally and chemically stable, while the other phases are in a metastable state and transform into β-phase at adequately high temperatures.

β-Ga_2O_3 has a wide bandgap of ~ 4.9 eV[3, 4] at RT. The lattice parameters of β-Ga_2O_3 were firstly estimated by Kohn *et al.*[5], and its structure was determined by Geller[1] in space group C2/m. Walton and Chase[6] clarified that the morphological symmetry appeared to be lower than that of the accepted point group 2/m.

As noted by Geller[1], there were several other interpretations regarding β-Ga_2O_3 but none had indicated a deviation from a monoclinic structure. Furthermore, an accurate investigation of the β-Ga_2O_3 crystal structure was presented by Ahman *et al.*[7] and Janowitz *et al.*[8]. The X-ray diffraction symmetry and refinement of the structure clearly indicted a C-centered monoclinic cell with space group C2/m. Fig. 1 presents a unit cell that contains two nonequivalent Ga atoms: one with tetrahedral Ga(I) and the other with octahedral Ga(II). The oxygen atoms are arranged in a distorted cubic closely packed array and have three non-equivalent oxygen ions [O (I), O (II), and O (III)] that are situated at 4i(x, 0, z) positions[9].

Thus far, the density functional theory (DFT) is the most suitable for calculating the electronic band structure of β-Ga_2O_3. Although, several theoretical studies on the electronic structure of β-Ga_2O_3 have been published[10–15], they presented a similar calculation for DFT (Fig. 2).

3. Ga_2O_3 growth methods

In this section, we present an overview of the bulk crystal growth of β-Ga_2O_3. The following are the most common methods of bulk Ga_2O_3 crystal growth:

·Verneuil method
·Floating zone (FZ) method
·Czochralski (CZ) method
·Edge-defined film-fed growth (EFG) method
·Bridgman method

Correspondence to: C T Xia, xia_ct@siom.ac.cn
Received 30 SEPTEMBER 2018; Revised 7 DECEMBER 2018.

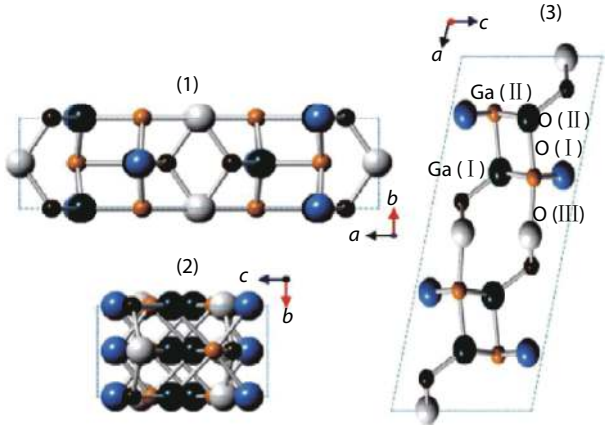

Fig. 1. (Color online) Unit cell of β-Ga_2O_3, which possesses two nonequivalent Ga sites: Ga (I), Ga (II), and three nonequivalent O-sites. Projection of the unit cell of β-Ga_2O_3 along the *c*- (A), *a*- (B) and *b*-axes (C). The figure was adopted from Ref. [9].

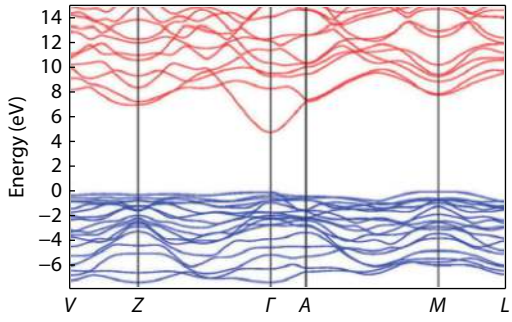

Fig. 2. (Color online) Electronic band structure of β-Ga_2O_3[15].

3.1. Verneuil method

The Verneuil method was developed by Auguste Verneuil in 1902 and is also known as flame fusion. This process is used mainly to fabricate the gem varieties of sapphire and ruby. The steps of the operation include melting the powder material using an oxyhydrogen flame, and thereafter, the melted material crystallizes into boule (as shown in Fig. 3).

In 1964, Chase[17] prepared the first β-Ga_2O_3 single crystal boules using the Verneuil method. The crystals grow to the desired size by increasing the gas flow and powder feed; the obtained boules are 3/8 inch in diameter and 1 inch in length. The growth direction of the boule was mostly parallel to the crystallographic *b* axis. β-Ga_2O_3 has two cleavage planes (100) and (001). Thin slabs of β-Ga_2O_3 can be prepared by slitting the crystal on these planes. In addition, β-Ga_2O_3 crystals in the direction [100] have a twin plane and the majority of the crystals exhibit fine laminar twinning.

In addition, Lorenz *et al.*[18] found that the Verneuil method permits a redox reaction in the growth process. β-Ga_2O_3 crystals were insulating and colorless when grown in an oxidizing condition. In contrast, crystals grown under reducing conditions were bluish. Mg- and Zr-doped β-Ga_2O_3 crystals were grown by Harwig *et al.*[19, 20] using the same method. They demonstrated that the crystals were light blue and blue when doped with Mg and Zr, respectively[19].

3.2. Floating zone (FZ) method

In 1955, Theurer[21] modified the method developed by Pfann at Bell Lab for germanium, which is known as the FZ method. This method relies on moving a liquid zone through

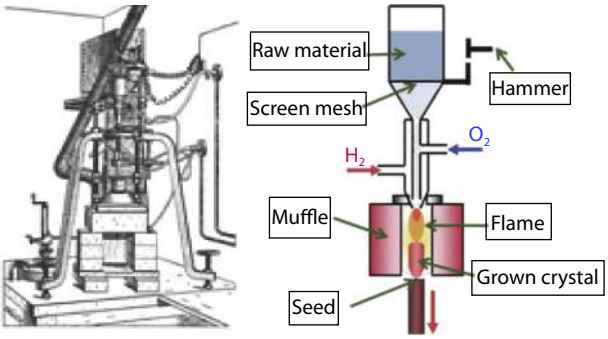

Fig. 3. (Color online) (a) Sketch of an early furnace used by Verneuil. (b) Simplified diagram of Verneuil process for synthesizing Ga_2O_3[16].

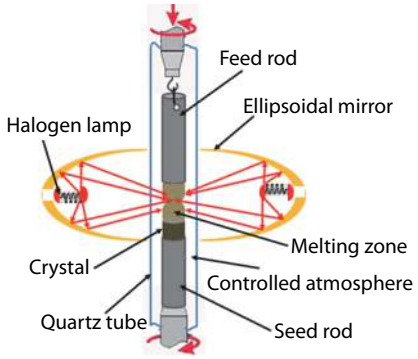

Fig. 4. (Color online) Schematic of float zone single crystal growth.

the material, and if properly seeded, a single crystal may be obtained, as shown in Fig. 4. The most prominent feature of this method is that no crucible is required, which facilitates the growth of congruent as well as incongruent melting materials.

Villora *et al.*[22] grew a single crystal β-Ga_2O_3 of approximately 1 inch in three crystallographic directions: [100], [010], and [001] (Fig. 5).

Moreover, Zhang *et al.* [23] grew crystals with a 6-mm diameter and 20-mm length using the same method and also found that the preferred crystallographic growth direction is <010>.

The major drawback of this method is that it is difficult to prevent the liquid from collapsing. It can only be held in place by surface tension. Cracks occur in the cooling crystal owing to the stress caused by high thermal gradients.

3.3. Czochralski method

The Czochralski method is a process of growing single crystals of metals (Pd, Pt, Ag, Au, etc.), semiconductors (Si, Ge, and GaAs), and artificial gemstones (Fig. 6).

In 1915, Czochralski invented this method while investigating the rate of metal crystallization[24]. The most prominent feature of this method is the growth of large boules or cylindrical ingots of a single crystal. Some scientists believe the Czochralski method is the "inverse" of the Verneuil technique. The following steps briefly describe the work process involved. High-purity material is melted within a crucible, and a seed on a rod is then immersed in the liquid. The rod is pulled upwards and rotated simultaneously.

The diameter of the crystal increased to approximately 2 inch. The growth direction is always along the <010> crystallographic direction, which is parallel to both cleavage planes (100) and (001).

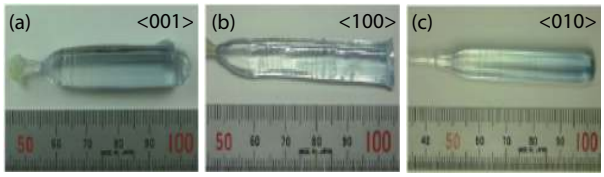

Fig. 5. (Color online) As-grown crystals along the crystallographic axis (a- <100>), (b- <010>), (c- <001>]).

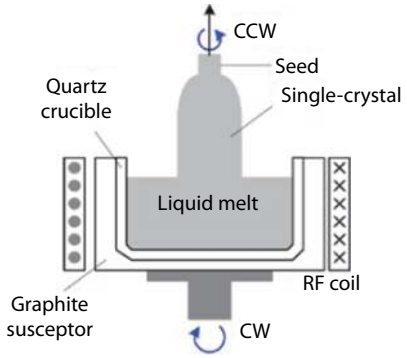

Fig. 6. Schematic of Czochralski method.

The first Czochralski growth of a β-Ga_2O_3 single crystal was reported by Tomm *et al.*[26]. They utilized 10% CO_2 in Ar instead of O_2 to decrease the evaporation of molten Ga_2O_3. Galazka *et al.*[25] utilized similar growth conditions to grow β-Ga_2O_3 crystals. They found that the CO_2 concentration in the growth atmosphere may be used for adjusting the crystal perfection and growth stability in addition to tuning the optical and electrical properties of the crystals. Galazka *et al.*[27] presented a new approach for scaling up the growth of β-Ga_2O_3 single crystals grown from the melt. They found that the desired larger crystal required a higher oxygen concentration in the growth atmosphere of up to 100 vol.%. They illustrated the growth of a cylindrical crystal with a 2-inch diameter (as shown in Fig. 7). When using an oxygen concentration between 8 and 35 vol.%

Furthermore, the same co-workers of Galazka in 2018[28] experimentally studied the segregation of Ce, Cr, Al-doped β-Ga_2O_3 crystals grown using the Czochralski method as well as the effect of doping on the optical properties. They observed that both the segregation and incorporation of Cr and Ce into the β-Ga_2O_3 crystals strongly depended on the O_2 concentration during the growth and on their charge state.

3.4. Edge-defined film-fed growth (EFG) method

Intensive experiments performed by La Belle and Mlavsky[29–31] on the growth of sapphire tubes resulted in the discovery of the edge-defined film-fed growth (EFG) technique. They observed that if the top surface of the shaper (also referred to as a die) was flat, the molten materials spread out to the edge and stopped, which implied that the melt wetted a die shaper. Hence, the diameter of the die, and not of the melt column, dictated the diameter of the filament produced (Fig. 8). Consequently, the technique was named "edge-defined film-fed growth". The major problems of this method are the geometry and the material of the die, while the major advantages of this method are the growth of a near-net shape and other complicated shapes and a higher growth rate. The growth direction was the [010] crystallographic direction, which is parallel to both the cleavage planes (100) and (001).

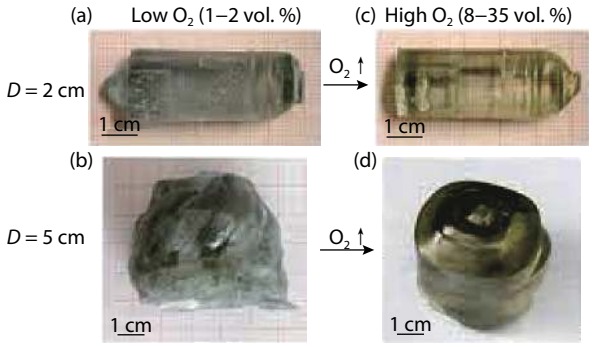

Fig. 7. (Color online) Semiconducting β-Ga_2O_3 crystals of 2 cm (a, c) and 5 cm (b, d) diameter grown at low- (a, b) and high-oxygen concentrations (c, d)[25].

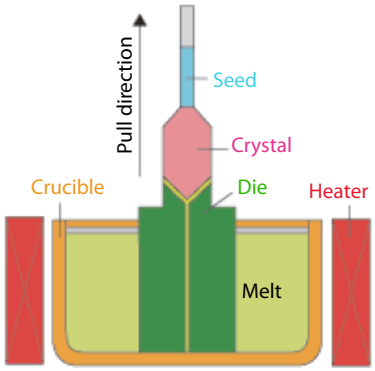

Fig. 8. (Color online) Edge-defined film-fed growth method.

The first successful growth of β-Ga_2O_3 single crystals using the EFG method was reported by Aida[32] *et al.* wherein the rate of growth was 10 mm/h for crystal ribbons with 50-mm width, 70-cm length, and 3-mm thickness. Mu *et al.*[33] grew bulk β-Ga_2O_3 single crystals having a width of 1 inch using an optimized EFG method under an Ar and 50% CO_2 atmosphere. The full width at half maximum of the X-ray rocking curve was only 43.2 arcsec, indicating high-quality single crystals.

Kuramata *et al.*[34] reported on the growth of large and high-quality β-Ga_2O_3 single crystals using the EFG method (Fig. 9(a)). They obtained a semiconductor substrate containing no twin boundaries with a diameter of up to 4 inches (Fig. 9(b)). The etch pit density revealed that the dislocation density on the $(\bar{2}01)$, (010), and (001) oriented wafers was in the order of 10^3 cm^{-2}. Moreover, Kuramata *et al.*[35] also showed the growth of large crystals of up to 6 inches by the EFG method.

Chinese scientists also used this method to grow bulk crystals, Zhang *et al.*[36] grew 2-inch crystal with an atmosphere of 20% argon (Ar) and 80% carbon dioxide (CO_2) (Fig. 9(c)), and FWHM of rocking curve was only 19.06 arcsec. Our group also reported 2-inch crystal growth (Fig. 9(d) published in CCCG-18 conference) .

3.5. Bridgman method (vertical or horizontal)

The Bridgman–Stockbarger method is named after the Harvard physicist, Percy Williams Bridgman (1882–1961) and MIT physicist, Donald C. Stockbarger (1895–1952)[37, 38]. This method depends on the directional solidification process controlled by the movement of the crucible containing the molten to the axial temperature gradient in a vertical/horizontal furnace. Initially, the polycrystalline material is required to be

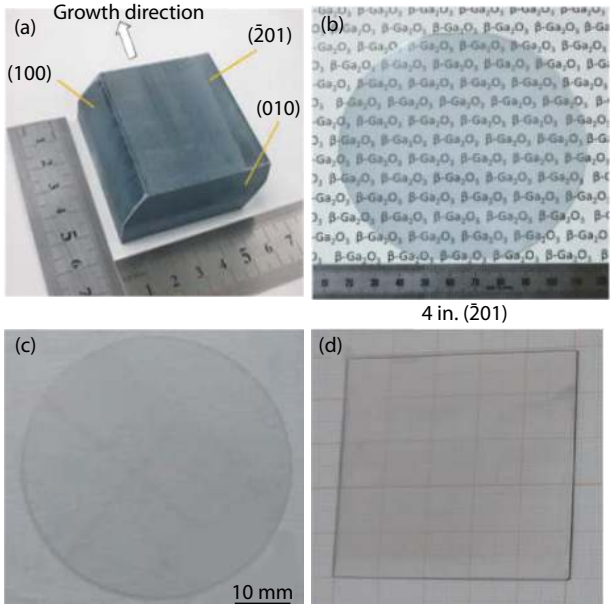

Fig. 9. (Color online) (a) Photograph of EFG-grown β-Ga_2O_3 bulk crystal. (b) Photographs of processed β-Ga_2O_3 substrates. (c) 2-inch wafer by Electronic Material Research Institute of Tianjin. (d) 2-inch plate by Shanghai Institute of Optics and Fine Mechanics.

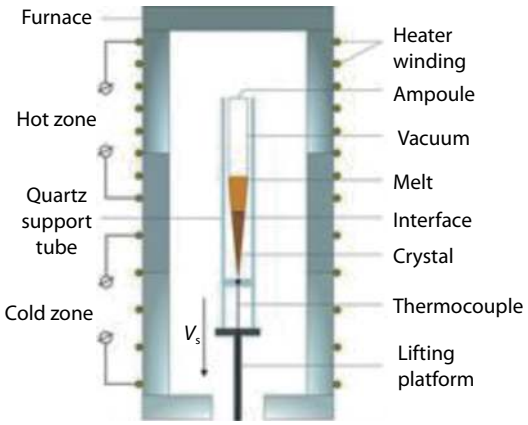

Fig. 10. (Color online) Bridgman technique.

melted completely in the hot zone, and then, it should be slowly cooled from the end of a seed crystal. A single crystal is gradually formed along the direction of the container length (Fig. 10).

Part of the seed will be re-melted after contact with the melt. One feature of this method of growing β-Ga_2O_3 is the utilization of a platinum–rhodium (70%–30%) crucible[39, 40], which can weather a high oxygen concentration.

Hoshikawa *et al.*[39] studied the effect of the crucible material on the shapes of the grown β-Ga_2O_3 crystals on using the vertical Bridgman (VB) method. They found that β-Ga_2O_3 single crystals were grown in the direction perpendicular to the (100) faceted plane using a seedless growth method in ambient air with a diameter of 25 mm and without adhering to the wall of the vertical cylinder crucible or a conical crucible (Fig. 11).

Ohba *et al.*[40] studied the structural defects on (100) wafers in β-Ga_2O_3 single crystals approximately 25 mm in diameter grown by directional solidification in a vertical Bridgman furnace. They observed no regions of high dislocation density near the periphery of the (100) wafers cut as cross sections from the crystal ingots. Moreover, they detected line-

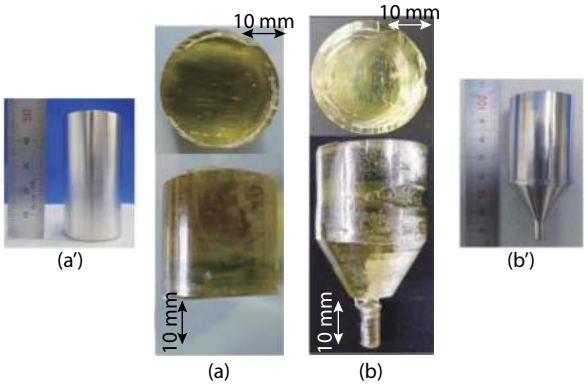

Fig. 11. (Color online) β-Ga_2O_3 crystals were grown using the VB method in ambient air. (a–a') Crystal was grown in a full-diameter crucible, and (b–b') crystal was grown in a conical crucible. The figure was adopted from Ref. [38].

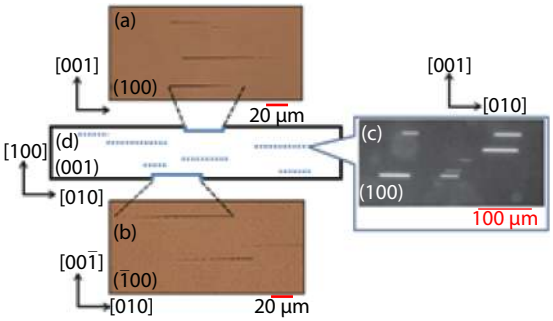

Fig. 12. (Color online) Schematics of line-shaped defects. The figure was adopted from Ref. [40].

shaped defects that were 20–150 μm in length in the <010> direction using optical microscopy, as shown in Fig. 12. These defects are considered to be the same as those observed in the previously used EFG method.

In summary, the crucible-free FZ and Verneuil methods facilitate the use of a high oxygen concentration and a reduced amount of residual impurities. The Czochralski method provides a large crystal size of approximately 2 inch in diameter, while the EFG method provides a 6-inch-width crystal of the highest quality.

Ga_2O_3 substrates underwent a massive breakthrough owing to their low cost and low energy consumption. The following organization chart (Fig. 13) depicts the comparison of the melt growth methods for β-Ga_2O_3 bulk single crystals.

In addition, the best method for the mass production of substrates is the EFG method, which has a good track of the availability of large area, low defect density, high crystal quality.

4. Doping of β-Ga_2O_3

The conductivity control through doping and the curtailing of the trap states is the solution to obtaining β-Ga_2O_3 for technological applications[41]. In this section, we present an overview of high-quality doping.

4.1. Donor doping of β-Ga_2O_3

4.1.1. Unintentional self-doping

A β-Ga_2O_3 crystal exhibits n-type conductivity with no intentional doping. The n-type semiconductivity is commonly attributed to oxygen vacancies, which are ionized and form donors. Therefore, it is assumed that there is a strong correlation

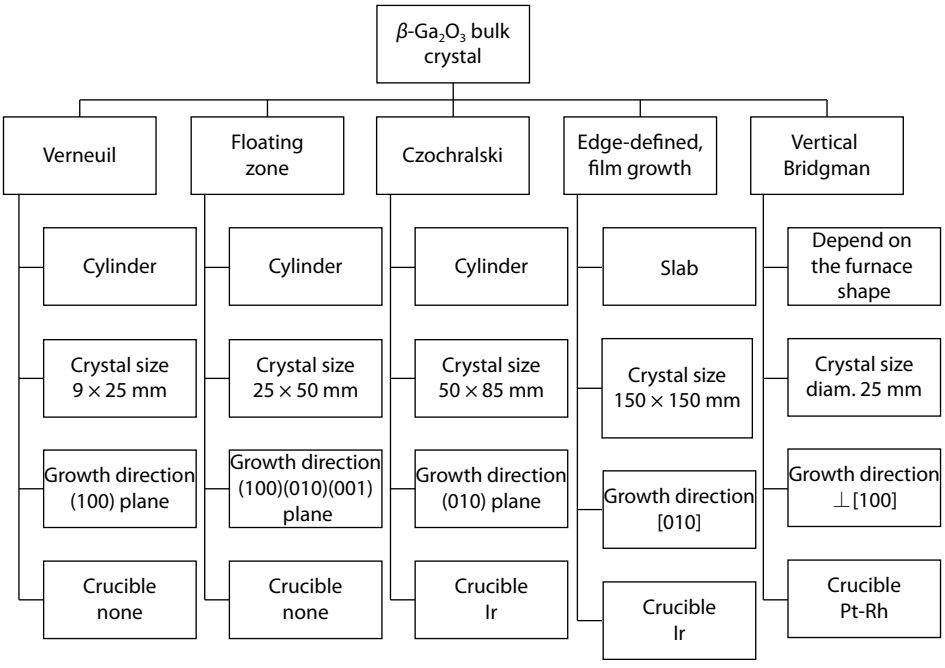

Fig. 13. The comparison of the melt growth methods for β-Ga_2O_3 bulk single crystals.

between the conductivity of β-Ga_2O_3 crystals and oxygen vacancies. This assumption has been debated by Varley *et al.*[15] who performed first-principle calculations for various impurities and oxygen vacancies in β-Ga_2O_3. Based on calculations, they suggested that the oxygen vacancy serves as a deep donor with an ionization energy of more than 1 eV and, thus, cannot contribute to n-type. They proposed that hydrogen is the probable cause of the electrical conductivity.

Zhang *et al.*[23] produced β-Ga_2O_3 single crystals using the FZ method. They found that the 300-nm emission can be ascribed to the potential wells formed by acceptor clusters, and the 692-nm emission was attributed to the recombination of holes and electrons via the acceptors and donors in the vicinity.

4.1.2. Intentional n-type doping

The fabrication and characterization of Sn-doped β-Ga_2O_3 single crystals were studied by Suzuki *et al.*[42] and Ueda *et al.*[43] via the FZ method. High-conductivity crystals were obtained using the FZ method using Ga_2O_3 rods doped with 2–10 mol% SnO_2. The low incorporation efficiency causes a massive amount of Sn atoms to evaporate during the growth process. Ueda *et al.*[43] reported that Sn-doped β-Ga_2O_3 had a blue coloration, and the value of their conductivity was 0.96 Ω^{-1} cm^{-1} (electrical resistivity = 1.04 Ω·cm). Suzuki *et al.*[42] reported that the optimized specimen was 32 ppm. The conductivity value is 23.4 Ω^{-1}·cm^{-1} (electrical resistivity = 4.27 × 10^{-2} Ω·cm), and the carrier concentration is approximately 2.26×10^{18} cm^{-3}. Zhang *et al.*[23] studied the effect of Sn doping in β-Ga_2O_3 crystals prepared using the FZ method and that of the annealing process on their conductivity and optical properties. They showed that the forbidden bandwidth of β-Ga_2O_3 is influenced by Sn^{4+} doping. Both the absorption coefficient and conductivity increase on increasing the Sn doping. A reduction in the absorption coefficient after the annealing refers to the decrease in the free carriers. Thus, the annealed process changes the sample into an insulator. Moreover, Ohira *et al.*[44] examined the effect of the annealing process on the surface morphology, electrical and optical properties of Sn-doped β-Ga_2O_3 produced using the FZ method. It was observed that these properties did not change, however the lattice parameters increased slightly after annealing at 1100 °C. Furthermore, Sn was uniformly dispersed in the β-Ga_2O_3 matrix.

Víllora *et al.*[45] obtained Si-doped β-Ga_2O_3 using the FZ method. It was found that the Si concentration is in the range of 10^{16}–10^{18} cm^{-3}, and the conductivity increases contentiously from 0.03 to 50 $\Omega^{-1}cm^{-1}$. At a low doping rate, nearly all the Si is incorporated into the crystals, while at a high doping rate, the Si concentration in the crystal is approximately 5% that of the feed rod. While the mobility fluctuated around 100 cm^2/V, the free carrier concentration increased by three orders of their magnitude. Therefore, the electrical conductivity depends sustainably on the main impurity. This is in agreement with the theoretical calculations[15], which shows that the oxygen vacancies in the crystal are deep donors and can hardly contribute to the electron conductivity.

Sasaki *et al.*[46] published good results on Si-ion implantation into Ga_2O_3 crystals fabricated using the FZ method. The Si concentration varies from 1×10^{19} to 1×10^{20} cm^{-3} owing to the varying in the total dose from 2×10^{14} to 2×10^{15} cm^{-2}. The sample with a Si concentration of 5×10^{19} cm^{-3} had a resistivity of 1.4 mΩ·cm. A high electrical activation efficiency of over 60% was obtained in the samples with a Si concentration of $\leqslant 5 \times 10^{19}$ cm^{-3} through the annealing process in the range of 900–1000 °C. Kuramata *et al.*[34] reported the growth of Si-doped β-Ga_2O_3 bulk crystals using the EFG and FZ methods and investigated the residual impurities, controllable doping, crystal defect, and the effect of thermal annealing on the electrical properties of the β-Ga_2O_3 bulk crystals. They observed that the main residual impurity in the EFG crystals is Si and that the Si content controlled the effect donor concentration ($N_d - N_a$) of unintentionally doped crystals. Therefore, obtaining an intentionally n-doped crystal was found to be possible by doping with SiO_2. $N_d - N_a$ was approximately the same as the Si concentration in the samples annealed in nitrogen,

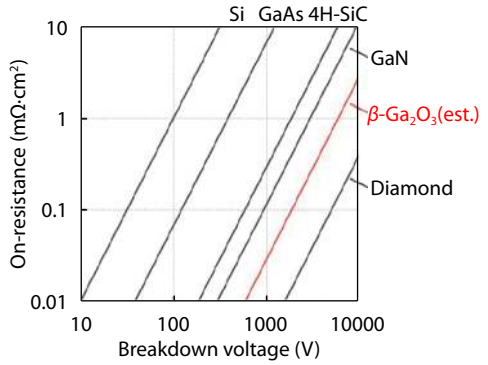

Fig. 14. (Color online) Theoretical ideal performance limits of β-Ga_2O_3 power devices in comparison with those of other major semiconductors. The figure was adopted from Ref. [58].

while it was independent of the Si concentration under oxygen ambient.

Zhou *et al.*[47] experimentally confirmed that Nb element is a good choice to control the conductivity of β-Ga_2O_3. Nb-doped β-Ga_2O_3 crystals were grown using the FZ method, and their structure was that of monoclinic β-Ga_2O_3. The electrical resistivity decreased from 3.6×10^2 to 5.5×10^{-3} Ω·cm and the carrier concentration increased from 9.55×10^{16} to 1.8×10^{19} cm^{-3} on increasing the doping.

4.2. Acceptor doping of β-Ga_2O_3

A major challenge for of β-Ga_2O_3 is its lack of an adequate method for fabricating p-type β-Ga_2O_3 crystals. Few reports on p-type Ga_2O_3 have been published[48].

4.2.1. Unintentional self-doping

Varley *et al.*[49] studied the effect of holes in many bandgap oxides and found that the holes in Ga_2O_3 can form self-trap holes with an energy of 0.53 eV. This indicates that free holes will be precarious and tend to localize as small polarons. Kananen *et al.*[50] observed self-trapped holes in Ga_2O_3 using the electron paramagnetic resonance technique. These defects are thermally stable below ~80–100 K.

4.2.2. Intentional p-type doping

Onuma *et al.*[51] obtained Mg-doped β-Ga_2O_3 crystals using the FZ method and found the samples' behavior to be semi-insulating with a resistivity of 6×10^{11} Ω·cm for Mg concentration of 4×10^{18}–2×10^{19} cm^{-3}. The Blue luminescence intensity depended on the Mg doping, and there was a correlation between the intensity and the formation energy of V_o. Mg-doped β-Ga_2O_3 crystals were prepared by Galazka *et al.*[27] via the CZ method in a very low range of Mg of 6–28 ppm at 100% CO_2, which indicates that Mg very efficiently compensates acceptors. Thus far, only Liu *et al.*[52] have reported on N-doped β-Ga_2O_3 nanowires with a p-type electrical conductivity. As in the case of β-Ga_2O_3, p-type doped ZnO is difficult to acquire, and previous studies have stated that N acceptors are strongly compensated by intrinsic defects, and N atoms cannot be effective acceptors owing to the deep acceptor levels in the bandgap of ZnO. Dong *et al.*[53] studied the compensation mechanism between N acceptors and native defects in β-Ga_2O_3 using first-principle calculations based on DFT. They found that the N dopant serves as a deep acceptor with an acceptor level of 1.33 eV above the valence band maximum, which cannot be an effective p-type dopant. In addition, the N dopant formed four types of defect complexes including oxygen and Gallium vacancies and interstitials. Kyrtsos *et al.*[54] used DFT to investigate the various cation substitutional dopants in β-Ga_2O_3 for the possibility of p-type conductivity. They found that these dopants act as deep acceptor levels with ionization energies of more than 1 eV. They can also trap an extra hole at a very deep donor level, which inhibits p-type conductivity.

5. Applications

In this section, we present an overview of the applications of β-Ga_2O_3.

5.1. Gas sensors

The working principle of oxygen sensor devices is a negative relationship between the conductivity of β-Ga_2O_3 and the oxygen partial pressure in the surrounding atmosphere. The conductivity of the sensor changes with varying the proportion of oxygen or the concentration of gases in the atmosphere. Bartic *et al.*[55] studied the oxygen sensitivity of Ga_2O_3 single crystals and thin films at high temperatures. They found that the difference in response times between a single crystal and poly material was small.

5.2. Power and high-voltage devices

The critical electric field can be determined from the bandgap using an empirical relationship[56]:

$$E_c = 1.73 \times 10^5 (E_g)^{2.5}$$

The estimated breakdown voltage is 8 MV/cm, which is approximately three times larger than that of SiC or GaN. The corresponding Baliga's Fig. of merit (BFOM $\propto \varepsilon\mu E_c^3$), which is used to estimate the potential for power device applications, is at least four times larger than those of SiC or GaN. Furthermore, the conduction loss of Ga_2O_3 is lower than that of other semiconductor materials[57, 58]. Thus, Ga_2O_3 is one of the most suitable materials for power-device applications. Fig. 14 shows a comparison of the theoretical performance limits of Ga_2O_3 with those of other major semiconductors.

5.3. Schottky diodes

High-performance Schottky barrier diodes were fabricated by Oishi *et al.*[59] on an EFG-grown β-Ga_2O_3 single crystal. The highest theoretical value of electron mobility reported thus far is 886 $cm^2/V{\cdot}s$ at 85 K. The current density was 70.3 A/cm^2 at 2.0 V for a forward voltage, and an ideality factor of 1.01 was obtained. Moreover, the Schottky barrier diodes fabricated using the FZ technique offered good characteristics, a high reverse breakdown voltage of approximately 150 V, and a barrier height of the Pt/β-Ga_2O_3 interface of 1.3–1.5 eV[60].

Recently, the highest performance of β-Ga_2O_3 Schottky barrier diode (SBD) was reported by Xidian University[61], with a reverse blocking voltage of more than 3 kV and a low DC specific ON-resistance (R_{ON},sp) of 24.3 mΩ·cm^2.

5.4. Field effect transistors (FET)

Higashiwaki *et al.*[62] first demonstrated an interesting design of a metal semiconductor field-effect transistor (MESFET) using Ga_2O_3 single crystals. They fabricated n-channel Ga_2O_3 MESFETs on a single-crystal Mg-doped β-Ga_2O_3 (010) substrate. A Sn-doped (100) semi-insulating β-Ga_2O_3 grown onto a Mg-doped β-Ga_2O_3 crystal was fabricated by Green *et al.*[63] using Metal organic chemical vapor deposition(MOCVD). They reported on Ga_2O_3 metal-oxide-semiconductor field effect tran-

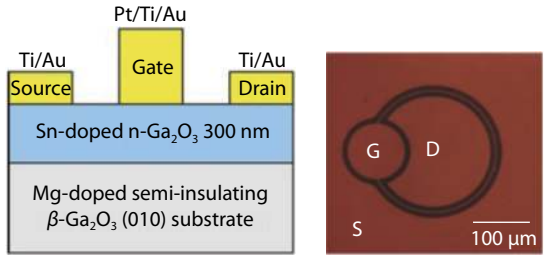

Fig. 15. (Color online) Schematic illustration: (a) cross-section and (b) optical micrograph of Ga_2O_3 MESFET. According to the description from Ref. [62].

sistors (MOSFETs) with a gate-to-drain electric field corresponding to 3.8 MV/cm, which is the highest reported for any transistor surpassing bulk GaN and SiC theoretical limits[62]. A cross-section of the Ga_2O_3 MESFET structure is shown in Fig. 15.

5.5. UV detectors

Photodetectors are one of the simplest devices to produce as they require only Schottky or Ohmic contacts. The major application of these devices is solar-blind ultraviolet (UV) radiation detection. Owing to its wide bandgap, Ga_2O_3 provides a unique opportunity for the detection of UV radiation of wavelengths <280 nm.

Suzuki *et al.*[64] fabricated β-Ga_2O_3 photodiodes with an Au Schottky contact on a single crystal substrate. They also investigated the effect of post heat treatment on the electrical and optical properties of photodiodes. The ideality factor improved to nearly 1 subsequent to annealing at temperatures greater than 200 °C; however, the reverse leakage current remained nearly unchanged. The high responsivity and bias-voltage dependence of the photocurrent implies the presence of an internal gain. Yang *et al.*[65] fabricated a Schottky barrier diode solar-blind photodetector based on a single crystal β-Ga_2O_3. They found that the device has a clear response to the solar-blind wavelength at a zero bias, which confirms that it can be used as a self-powered solar-blind photodetector.

5.6. Radiation detection

Wide bandgap semiconductors feature strong bonds that provide them with an intrinsically high radiation resistance[41]. Patrick *et al.*[66] investigated Ga_2O_3 as a radiation detection material for fast (14 MeV) neutrons, using the ^{16}O (n, α) ^{13}C reaction. Yang *et al.*[67] exposed vertical rectifiers fabricated on epi Ga_2O_3 on bulk β-Ga_2O_3 to 1.5-MeV electron irradiation at fluences from 1.79×10^{15} to 1.43×10^{16} cm^{-2} at a fixed beam current of 10^{-3} A. The electron irradiation led to a reduction in the carrier concentration of Ga_2O_3 with a carrier removal rate of 4.9 cm^{-1}. Szalkai *et al.*[68] illustrated the capability of Mg-doped β-Ga_2O_3 single crystals in detecting fast neutrons. They observed a gamma signal from a Ga decay process when a neutron-irradiated β-Ga_2O_3 crystal sample was tested using a high-purity germanium detector.

6. Conclusions and future perspectives

This review summaries the state of the art of β-Ga_2O_3 and achievements with respect to β-Ga_2O_3 ranging from preparation and characterization to applications. Although significant progress has been made in the growth of bulk crystals, defect and impurity control require further studies. As can be observed from this article, the published data on Ga_2O_3 are still incomplete and controversial to some extent. We look forward to realizing the following objectives that may be important research and development paths with respect to β-Ga_2O_3 bulk-based devices.

(1) Identification of the dominant defects in bulk crystals and their effect on device performance

(2) Experimental efforts to address open issues such as p-type conductivity and realizing the full potential of Ga_2O_3 materials in device applications

(3) New concepts and designs for improving the thermal management and reliability of power electronics devices

(4) Further progress in growth of large-diameter high-quality crystals

Acknowledgments

This work is funded by the following grants: Chinese Academy of Sciences president's International Fellowship Initiative (Grant No. 2018PE0033), National Natural Science Foundation of China (Grant No. 51802327), Science and Technology Commission of Shanghai Municipality (No. 18511110500), and Pre-research Fund Key Project (No. 6140922010601) .

References

[1] Geller S. Crystal structure of β-Ga_2O_3. J Chem Phys, 1960, 33, 676
[2] Roy R, Hill V G, Osborn E F J. Polymorphism of Ga_2O_3 and the System Ga_2O_3–H_2O. Am Chem Soc, 1952, 74, 719
[3] Tippins H H. Optical absorption and photoconductivity in the band edge of β–Ga_2O_3. Phys Rev, 1965, 140, A316
[4] Hajnal Z, Miro J, Kiss G, et al. Role of oxygen vacancy defect states in the n-type conduction of β-Ga_2O_3. J Appl Phys, 1999, 86, 3792
[5] Kohn J A, Katz G, Broder J D. Characterization of β-Ga_2O_3 and its alumina Isomorph θ-Al_2O_3. Am Minerol, 1956, 42, 398
[6] Wolten G M, Chase A B. Determination of the point group of β-Ga_2O_3 from morphology and physical properties. J Solid State Chem, 1976, 16, 377
[7] Ahman J, mSvensson G, Albertsson J. A reinvestigation of β-gallium oxide. Acta Crystallogr Sect C Cryst Struct Commun, 1996, 52, 1336
[8] Janowitz C, Scherer V, Mohamed M, et al. Experimental electronic structure of In_2O_3 and Ga_2O_3. New J Phys, 2011, 13, 085014
[9] Yoshioka S, Hayashi H, Kuwabara A, et al. Structures and energetics of Ga_2O_3 polymorphs. J Phys Condens Matter, 2007, 19, 346211
[10] Yamaguchi K. First principles study on electronic structure of β-Ga_2O_3. Solid State Commun, 2004, 131, 739
[11] He H, Orlando R, Blanco M, et al. First-principles study of the structural, electronic, and optical properties of Ga_2O_3 in its monoclinic and hexagonal phases. Phys Rev B, 2006, 74, 195123
[12] Zhang Y, Yan J, Zhao G, et al. First-principles study on electronic structure and optical properties of Sn-doped β-Ga_2O_3. Physical B Condens Matter, 2010, 405, 3899
[13] Zhang L, Yan J, Zhang Y, et al. First principles study on electronic structure and optical properties of N-doped P-type β-Ga_2O_3. Sci China Phys, Mech Astron, 2012, 55, 19
[14] Peelaers H, Van de Walle C G. Brillouin zone and band structure of β-Ga_2O_3. Phys Status Solidi B, 2015, 252, 828
[15] Varley J B, Weber J R, Janotti A, et al. Oxygen vacancies and donor impurities in β-Ga_2O_3. Appl Phys Lett, 2010, 97, 142106
[16] Nassau K. Dr. A. V. L. Verneuil: The man and the method. J of Cry Growth, 1972, 13, 12
[17] Chase A B. Growth of β-Ga_2O_3 by the Verneuil technique. J Am

Ceram Soc, 1964, 47, 470
[18] Lorenz M R, Woods J F, Gambino R J. Some electrical properties of the semiconductor β-Ga_2O_3. J Phys Chem Solids, 1967, 28, 403
[19] Harwig T, Schoonman J. Electrical properties of β-Ga_2O_3 single crystals. J Solid State Chem II, 1978, 23, 205
[20] Harwig T, Wubs G J, Dirksen G J. Electrical properties of β-Ga_2O_3 single crystals. Solid State Communications, 1976, 18, 1223
[21] Theurer H C. Method of processing semiconductive materials. U. S. Patent 3,060,123 (Filed December 17, 1952. Issued October 23, 1962)
[22] Víllora E G, Shimamura K, Yoshikawa Y, et al. Large-size β-Ga_2O_3 single crystals and wafers. Journal of Crystal Growth, 2004, 270, 420
[23] Zhang J, Li B, Xia C, et al. Growth and spectral characterization of β-Ga_2O_3 single crystals. Journal of Physics and Chemistry of Solids, 2006, 67, 2448
[24] Czochralski J. A new method for the measurement of the crystallization rate of metals. Zeitschrift für Physikalische Chemie, 1918, 92, 219
[25] Galazka Z, Uecker R, Irmscher K, et al. Czochralski growth and characterization of β-Ga_2O_3 single crystals. Cryst Res Technol, 2010, 45, 1229
[26] Tomm Y, Reiche P, Klimm D, et al. Czochralski grown Ga_2O_3 crystals. J Cryst Growth, 2000, 220, 510
[27] Galazka Z, Uecker R, Klimm D, et al. Scaling-Up of Bulk β-Ga_2O3 Single Crystals by the Czochralski Method. ECS Journal of Solid State Science and Technology, 2017, 6, Q3007
[28] Galazka Z, Ganschow S, Fiedler A, et al. Doping of Czochralski-grown bulk β-Ga_2O_3 single crystals with Cr, Ce and Al. J Cry Growth, 2018, 486, 82
[29] LaBelle H E, Chalmers B, Mlavsky A I. Growth of controlled profile crystals from the melt: Part III — Theory. Mater Res Bull, 1971, 6, 681
[30] LaBelle H, Mlavsky A. Growth of controlled profile crystals from the melt: Part I - Sapphire filaments. Materials Research Bulletin, 1971, 6, 571
[31] LaBelle Jr H. Growth of controlled profile crystals from the melt: Part II - Edge-defined, film-fed growth (EFG). Materials Research Bulletin, 1971, 6, 581
[32] Aida H, Nishiguchi K, Takeda H, et al. Growth of β-Ga_2O_3 single crystals by the edge-defined, film fed growth method. Japanese Journal of Applied Physics, 2008, 47, 8506
[33] Mu W, Jia Z, Yin Y, et al. High quality crystal growth and anisotropic physical characterization of β-Ga_2O_3 single crystals grown by EFG method. Journal of Alloys and Compounds, 2017, 714, 453, 458
[34] Kuramata A, Koshi K, Watanabe S, et al. High-quality β-Ga_2O_3 single crystals grown by edge-defined film-fed growth. Jpn J Appl Phys, 2016, 55, 1202A
[35] Kuramata A, Koshi K, Watanabe Sh, et al. Bulk crystal growth of Ga_2O_3. Proc SPIE 10533, Oxide-based Materials and Devices IX, 2018, 105330E
[36] Zhang S N, Lian X Z, Ma Y C, et al. Growth and characterization of 2-inch high quality β-Ga_2O_3 single crystals grown by EFG method. J Semicond, 2018, 39, 083003
[37] Bridgman P W. Certain physical properties of single crystals of tungsten, antimony, bismuth, tellurium, cadmium, zinc, and tin. Proceedings of the American Academy of Arts and Sciences, 1925, 60, 305
[38] Stockbarger D C. The production of large single crystals of lithium fluoride. Review of Scientific Instruments, 1936, 7, 133
[39] Hoshikawa K, Ohba E, Kobayashi T, et al. Growth of β-Ga_2O_3 single crystals using vertical Bridgman method in ambient air. Journal of Crystal Growth, 2016, 447, 36
[40] Ohba E, Kobayashi T, Kado M, et al. Defect characterization of β-Ga_2O_3 single crystals grown by vertical Bridgman method. Jpn J Appl Phys, 2016, 55, 1202BF
[41] Tsao J Y, Chowdhury S, Hollis M A, et al. Ultrawide-Bandgap Semiconductors: Research Opportunities and Challenges. Adv. Electron Mater, 2018, 4, 1600501
[42] Suzuki N, Ohira S, Tanaka M, et al. Fabrication and characterization of transparent conductive Sn-doped β-Ga_2O_3 single crystal. Phys Status Solidi (C), 2007, 4, 2310
[43] Ueda N, Hosono H, Waseda R, et al. Synthesis and control of conductivity of ultraviolet transmitting single crystals. Appl Phys Lett, 1997, 70, 3561
[44] Ohira S, Suzuki N, Arai N, et al. Characterization of transparent and conducting Sn-doped β-Ga_2O_3 single crystal after annealing. Thin Solid Films, 2008, 516, 5763
[45] Víllora E G, Shimamura K, Yoshikaw Y, et al. Electrical conductivity and carrier concentration control in by Si doping. Appl Phys Lett, 2008, 92, 202120
[46] Sasaki K, Higashiwaki M, Kuramata A, et al. Si-ion implantation doping in β-Ga_2O_3 and its application to fabrication of low-resistance ohmic contacts. Appl Phys Express, 2013, 6, 6502
[47] Zhou W, Xia C, Sai Q, et al. Controlling n-type conductivity of β-Ga_2O_3 by Nb doping. Appl Phys Lett, 2017, 111, 242103
[48] Mastro M A, Kuramata A, Calkins J, et al. Perspective—opportunities and future directions for Ga_2O_3. J Solid State Sci Technol, 2017, 6, P356
[49] Varley J B, Janotti A, Franchini C, et al. Role of self-trapping in luminescence and-type conductivity of wide-band-gap oxides. Phys Rev B, 2012, 85, 081109
[50] Kananen B E, Halliburton L E, Stevens K T, et al. Gallium vacancies in β-Ga_2O_3 crystals. Appl Phys Lett, 2017, 110, 202104
[51] Onuma T, Fujioka S, Yamaguchi T, et al. Correlation between blue luminescence intensity and resistivity in β-Ga_2O_3 single crystals. Appl Phys Lett, 2013, 103, 2013
[52] Liu L L, Li M K, Yu D Q, et al. Fabrication and characteristics of N-doped β-Ga_2O_3 nanowires. Appl Phys A, 2010, 98, 831
[53] Dong L, Jia R, Li C, et al. Ab initio study of N-doped β-Ga_2O_3 with intrinsic defects: the structural, electronic and optical properties. J Alloys Compd, 2017, 712, 379
[54] Kyrtsos A, Matsubara M, Bellotti E. On the feasibility of p-type Ga_2O_3. Appl Phy Lett, 2018, 112, 032108
[55] Bartic M, Toyoda Y, Baban C I, et al. Oxygen sensitivity in gallium oxide thin films and single crystals at high temperatures. Jpn J Appl Phys, 2006, 45, 5186
[56] Hudgins J L, Simin G S, Santi E, et al. An assessment of wide bandgap semiconductors for power devices. IEEE Trans Power Electron, 2003, 18, 907
[57] Higashiwaki M, Sasaki K, Murakami H, et al. Recent progress in Ga_2O_3 power devices. Semiconductor Science and Technology, 2016, 31, 034001
[58] Higashiwaki M, Sasaki K, Kuramata A, et al. Development of gallium oxide power devices. Physica Status Solidi (a), 2014, 211, 21
[59] Oishi T, Koga Y, Harada K, et al. High-mobility β-Ga_2O_3(201) single crystals grown by edge-defined film-fed growth method and their Schottky barrier diodes with Ni contact. Appl Phys Express, 2015, 8, 031101
[60] Sasaki K, Higashiwaki M, Kuramata A, et al. Ga_2O_3 Schottky barrier diodes fabricated by using single-crystal β-Ga_2O_3(010) substrates. IEEE Electron Device Lett, 2013, 34, 493
[61] Hu Z Z, Zhou H, Feng Q, et al. Field-plated lateral β-Ga_2O_3 Schottky barrier diode with high reverse blocking voltage of more than 3 kV and high DC power figure-of-merit of 500 MW/cm^2. IEEE Electron Device Letters, 2018, 39, 1564
[62] Higashiwaki M, Sasaki K, Kuramata A, et al. Gallium oxide (Ga_2O_3) metal-semiconductor field-effect transistors on single-crystal β-Ga_2O_3 (010) substrates. Applied Physics Letters, 2012, 100, 013504
[63] Green A J, Chabak K D, Heller E R, et al. 3.8-MV/cm breakdown

strength of MOVPE-grown Sn-doped β-Ga_2O_3 MOSFETs. IEEE Electron Device Lett, 2016, 37, 902

[64] Suzuki R, Nakagomi S, Kokubun Y, et al. Enhancement of responsivity in solar-blind photodiodes with a Au Schottky contact fabricated on single crystal substrates by annealing. Appl Phys Lett, 2009, 94, 222102

[65] Yang C, Liang H, Zhang Z, et al. Self-powered SBD solar-blind photodetector fabricated on the single crystal of β-Ga_2O_3. RSC Adv, 2018, 8, 6341

[66] Patrick E, Choudhury M, Ren F, et al. Simulation of radiation effects in AlGaN/GaN HEMTs. ECS J Solid State Sci Technol, 2015, 4, Q21

[67] Yang J, Ren F, Pearton S J, et al. A 1.5 MeV electron irradiation damage in β-Ga_2O_3 vertical rectifiers. J Vac Sci Technol B, 2017, 35, 031208

[68] Szalkai D, Galazka Z, Irmscher K, et al. β-Ga_2O_3 solid-state devices for fast neutron detection. IEEE Trans Nucl Sci, 2017, 64(6), 1248